Effect of Cooling on the Probe System Sensitivity for Low Signal Strength RFI Problems

Guang-Hua Li [#1], Wei Huang [*2], David Pommerenke [#3]

[#] *EMC Laboratory, Missouri University of Science and Technology*
4000 Enterprise Dr. Rolla, MO, USA

[1]glbm4, [3]davidjp@mst.edu

[*] *ESDEMC Technology LLC*
4000 Enterprise Dr. Rolla, MO, USA

[2]whuang@esdemc.com

Abstract—**Only highly sensitive probe systems can detect the weak field strengths that cause radio-frequency-interference (RFI) problems typically found within cell phones. The sensitivity of the probe systems depends on the probe factor and on the noise floor. The effect of cooling by liquid nitrogen on the received signal strength and the noise floor of three resonant probe systems has been investigated. They operate at the GSM, GPS, and WiFi frequency bands. Cooling increases the Q-factor of these resonant probes, increases the received signal, and lowers the noise floor. The sensitivity of the system, defined as the signal strength at which the Signal-to-Noise Ratio is equal to 0 dB improves by 3-6 dB.**

***Keywords*— Quality factor, radio-frequency interference (RFI), resonant magnetic field probe, signal-to-noise ratio.**

I. INTRODUCTION

High-frequency harmonics generated from the digital ICs and switched power supplies may couple into the antennas which are integrated into mobile systems such as cell phones. The noise of the harmonics is added to the natural noise floor of the receiver and overwhelms weak signals which should be received by the receiver [1], [2]. Near-field probes [3], [4] and scanning technique are effective tools to investigate noise field distribution of circuits at high frequency and to locate the source of the EMI problems at circuit and chip level [5], [6].

Broadband probes are useful tools for initially locating strong noise sources. Magnetic near-field probes for high frequency band up to tens of GHz have been designed by suppressing the inherent resonances of a circular loop [7], and by minimizing the cross-sensitivity of electric near-field [8]. However, when the interfering electromagnetic fields are weak, it is difficult for broadband probes to measure signals of low signal-to-noise ratio (SNR). Probes with larger loop size can improve the SNR but degrade the spatial resolution. Since the noise source of interest is usually in the narrow bands, narrowband resonant probes can detect lower SNR signals than their broadband counterparts because of their higher sensitivity [9], [10]. In the applications of nuclear magnetic resonance (NMR), the SNR is further improved by lowering the coil temperature with liquid helium, since the noise is dominated by the thermal noise of the receiver coil in a well-designed NMR spectrometer [11], [12].

In the following paper, three resonant magnetic field probes are cooled with liquid nitrogen to investigate the effect of cooling on the probe system sensitivity, where only the probes are cooled. The probes operate at the GSM, GPS, and WiFi frequency bands. The sensitivity is defined as the signal at which the SNR reaches 0 dB within a bandwidth of 1 Hz. The experiment and results are described in detail in the following sections.

II. PROBE UNDER INVESTIGATION

The probe for investigating the effect of cooling is based on a differential-loop resonator shown in Fig. 1 and a Marchand balun based impedance transformer shown in Fig. 2. The theory, design and the dimension of the probe have been introduced in detail in [10]. The probe uses a four-layer FR4 printed circuit board. The initial design selected FR4 as substrate due to its low cost. The top and bottom layers in Fig. 1 are signal return planes and shielding planes minimizing unwanted field coupling. The LC resonator consists of a parallel-plate capacitor in parallel with an inductor formed by the probe loops. The resonant frequency of the probe is set by the geometry of the loops and the capacitors. The resonator is terminated with a Marchand balun based impedance transformer. The impedance transformer converts a high impedance Z_l of 1800 Ω to a low impedance Z_0 of 50 Ω. The high impedance is loading the resonator but allowing for a high Q-factor. The low impedance matches to the input impedance of measurement instruments such as the spectrum analyzer for maximal energy transfer. The transformer also converts differential signals to a single-ended signal, where the differential signals originate from the mirror-symmetrical design of the resonators on the second and third layers. Drawing of the fabricated resonant magnetic field probe at GPS frequency band are shown in Fig. 3. The assembled probe is about 6.5 cm long from the SMA connectors to the probe tip.

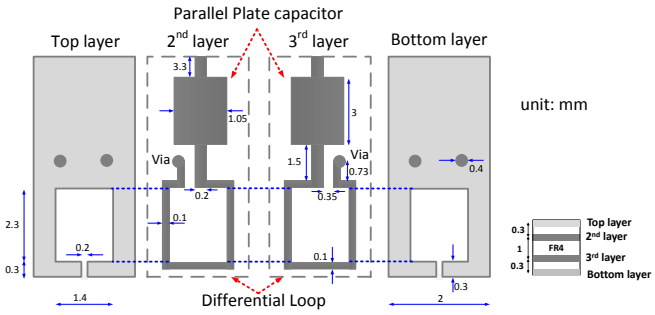

Fig. 1. Dimensions of the differential-loop resonator for the GPS probe. The differential loop is located at the tip of the resonator and then connected to the parallel-plate capacitor. The resonators of GSM and WiFi probes are similar.

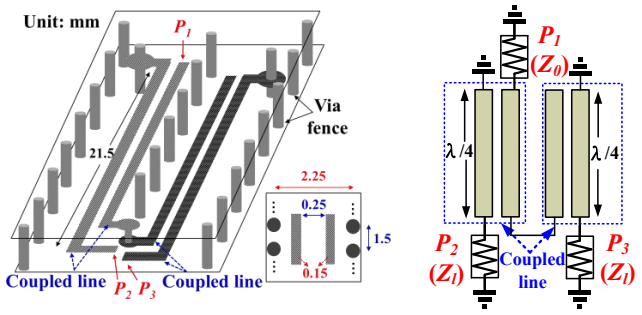

(a) (b)

Fig. 2. (a) Dimensions and (b) equivalent circuit of the Marchand balun for the GPS probe. The baluns of GSM and WiFi probes are similar.

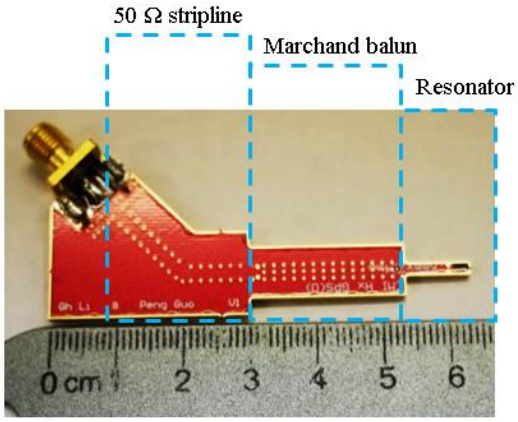

Fig. 3. Picture of the magnetic field GPS probe. The pictures of GSM and WiFi probes are similar.

III. Measurement Setup

Fig. 4 shows the measurement setup for investigating the effect of cooling probes by liquid nitrogen. The tracking generator of the spectrum analyzer outputs a sweeping sinusoidal signal to drive the 50 Ω microstrip trace terminated by a matched load. The probes are placed 2 mm (H = 2 mm, in Fig. 4) above the trace. This height is in the same order of the height commonly used in the near field scanning. The signal is amplified by a three-stage amplifier and then received by the spectrum analyzer. The amplifiers are connected to the probe output port directly.

The first stage amplifier, Amp1, is a narrow band low noise amplifier (LNA). The second and third stage amplifiers, Amp2 and Amp3, are broadband. The noise figures and gains are listed in Table I at the frequency bands of interest. The system noise figure attributed to the noise contribution of each stage amplifier in the cascade follow the Friis equation:

$$NF = NF_1 + \frac{NF_2 - 1}{G_1} + \frac{NF_3 - 1}{G_1 G_2} \quad (1)$$

where NF is the system noise figure, NF_i (i=1, 2, 3) is the noise figures of three amplifiers, and G_i (i=1, 2, 3) is the gain of three amplifiers. All the probes are matched to 50 Ω at their center frequencies. Therefore, the noise figure of amplifiers measured in a 50 Ω system is a reasonable estimate for calculation in Eqn. 1. All the values in Eqn. 1 are linear scale, not in decibels. The system noise figures are 0.6 dB, 0.9 dB, and 1.1 dB for GSM, GPS, and WiFi frequency bands, respectively. The system noise figure is mainly influenced by the LNA, which has a low noise figure and relatively high gain.

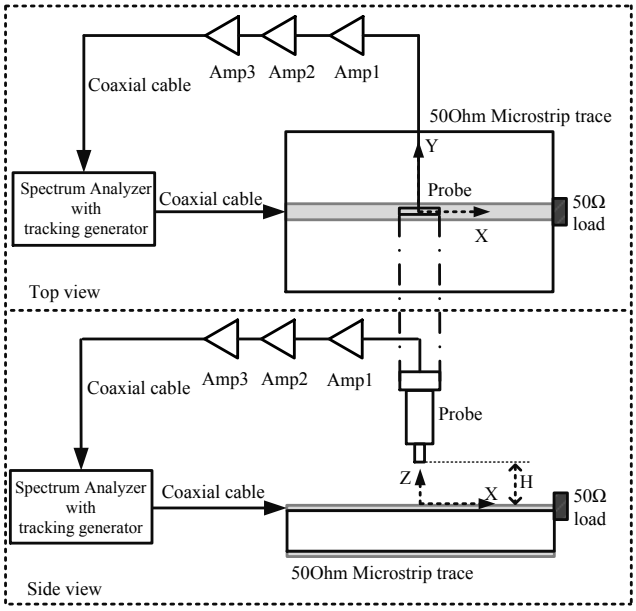

Fig. 4. Measurement setup for investigating the effect of cooling on the Q-factor, noise floor and sensitivity.

TABLE I
AMPLIFIERS USED IN THE MEASUREMENT

	Amp1	Amp2 and Amp 3	*NF*
GSM Probe	ZX60-1215LN+ (NF_1 = 0.4 dB) (G_1 = 17 dB)	ZX60-1412+ ($NF_{2\ or\ 3}$ = 5 dB) ($G_{2\ or\ 3}$= 11 dB)	0.6 dB
GPS Probe	ZX60-1614LN (NF_1 = 0.5 dB) (G_1 = 13 dB)	ZX60-1412+ ($NF_{2\ or\ 3}$ = 4.9 dB) ($G_{2\ or\ 3}$ = 11 dB)	0.9 dB
WiFi Probe	ZX60-272LN+ (NF_1 = 0.8 dB) (G_1 = 14 dB)	ZX60-1412+ ($NF_{2\ or\ 3}$ = 4.8 dB) ($G_{2\ or3}$ = 12 dB)	1.1 dB

IV. Cooling Effect on the Probe Q-factor

The probe's Q-factor was measured at room temperature and after cooling the probe in the liquid nitrogen. Although liquid nitrogen is not readily available in a real-word EMC laboratory at present, it is easy to buy a tank of liquid nitrogen. One might pour the liquid nitrogen onto the probe using a pipe during the real-world measurement. In the initial test, however, the probe is immersed in nitrogen. During the cooling, only the PCB of the probe has been placed into the liquid nitrogen for three minutes. The probe can stay cold for approximately two minutes after it is taken out from the liquid nitrogen. Then the probe was placed 2 mm (H = 2 mm) above the trace to measure signals, as shown in Fig. 4.

Cooling the probe increases the resonance frequencies (see Fig. 5). Take the GPS probe as an example. The resonance frequency increases by 46 MHz. The 3 dB bandwidth decreases by 29 MHz. The probe's Q-factor, Q, is calculated by

$$Q = \frac{f_c}{BW_{3dB}} \tag{2}$$

where f_c is the center frequency of the resonance, BW_{3dB} is the 3 dB bandwidth. The Q-factor when the probe is at room temperature is 11.3. After the cooling, the Q-factor is 14.7. The Q-factor increases by 3.4. Similar results for GSM and WiFi probes are listed in Table II. Both a small increase in the resonance frequency, and lower losses result in an increase of the Q-factor.

From the power point of view, the power received by the spectrum analyzer increases by 1-3 dB at the center frequency. At the same time, the loss in the probe reduces. The thermal noise in the conductors for the signal traces and the ground planes decreases with decreasing temperature. The dissipated power becomes smaller, leading to the higher Q-factor.

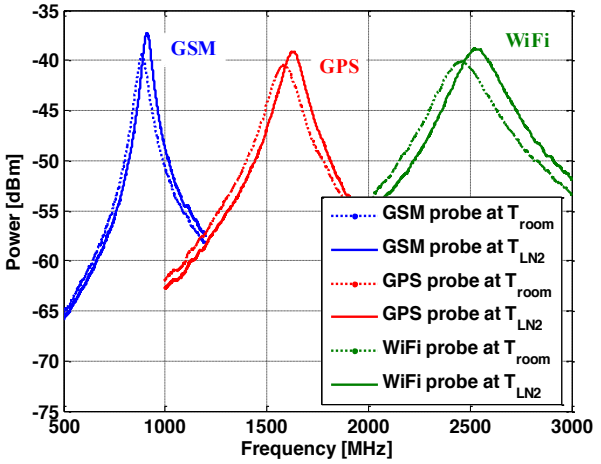

Fig. 5. Variation of the Q-factor for the GSM, GPS, and WiFi probes. T_{room} indicates room temperature. T_{LN2} indicates that the probe is cooled with liquid nitrogen.

TABLE II
Variations of the Probe's Q-factors when the Probe is at Room Temperature and Cooled with Liquid Nitrogen

		T_{room}	T_{LN2}	Difference
GSM Probe	f_c	885.7 MHz	909.5 MHz	23.8 MHz
	Power at f_c	-39.44 dBm	-37.3 dBm	2.14 dB
	BW_{3dB}	58.4 MHz	46.9 MHz	11.5 MHz
	Q-factor	15.2	19.4	4.2
GPS Probe	f_c	1581 MHz	1627 MHz	46 MHz
	Power at f_c	-40.49 dBm	-39.11 dBm	1.38 dB
	BW_{3dB}	140 MHz	111 MHz	29 MHz
	Q-factor	11.3	14.7	3.4
WiFi Probe	f_c	2452 MHz	2525 MHz	73 MHz
	Power at f_c	-40.2 dBm	-38.85 dBm	1.35 dB
	BW_{3dB}	237 MHz	212 MHz	25 MHz
	Q-factor	10.3	11.9	1.6

V. Equivalent Magnetic Field Strength of Noise Floor

The minimal detectable signal can be defined as the signal at which the SNR reaches 0 dB within a bandwidth of 1 Hz, when the noise power is equal to the noise power density. Real bandwidths are much larger. However, it is easy to denormalize to any requested bandwidth from 1 Hz. To calculate the noise equivalent signal, the system probe factor, SPF, and the noise power density, $P_{n,r}$, at the output of the probe system is needed. The noise power density is read directly from spectrum analyzer R&S FSV. The system probe factor is obtained from calibration.

During the calibration, the matched microstrip trace is driven by a source with a power level of P_d at the resonance frequency f_c. The input impedance looking into the microstrip trace at the driving port is R_{in} = 50 Ω. The voltage at the driving port is

$$V_d = \sqrt{P_d R_{in}}\ [V] \tag{3}$$

The microstrip trace generates a magnetic field, which is measured by the probes. The probes output a power, P_r, to the spectrum ananlyzer. Since the input impedance of the spectrum analyzer is R_{SA} = 50 Ω, the receiving voltage measured by the spectrum analzyer is

$$V_r = \sqrt{P_r R_{SA}}\ [V] \tag{4}$$

Therefore, the voltage transfer coefficient T_V from the driving voltage V_d to the receiving voltage V_r is

$$T_V = \frac{V_r}{V_d} = \frac{\sqrt{P_r R_{SA}}}{\sqrt{P_d R_{in}}} = \sqrt{\frac{P_r}{P_d}}\Bigg|_{R_{in}=R_{SA}=50\Omega} \tag{5}$$

We simulated the same matched microstrip trace driven by one Volt, and the magnetic field above the trace normalized to one Volt is H_{ref} in unit of (A/m)/V. In the measurement, the trace is driven by a voltage of V_d. The magnetic field strength, H_m, measured by the probe would be

$$H_m = H_{ref} V_d = H_{ref} \frac{V_r}{T_V} = H_{ref} V_r \sqrt{\frac{P_d}{P_r}} [A/m] \tag{6}$$

The system probe factor, SPF, is defined as:

$$SPF \triangleq \frac{H_m}{V_r} = H_{ref}\sqrt{\frac{P_d}{P_r}} \ [(A/m)/V] \quad (7)$$

Once the system probe factor *SPF* is known, the magnetic field strength H_m can be calculated if the receiving voltage V_r is given. When the SNR of the signal probe measures is 0 dB, the probe outputs a noise power of $P_{n,r}$ within a bandwidth of 1 Hz. The voltage measured by the spectrum analyzer then is

$$V_r = \sqrt{P_{n,r}R_{SA}} \ [V/\sqrt{Hz}] \quad (8)$$

The equivalent magnetic field strength of the noise is

$$H_{eq} = SPF \cdot V_r = SPF \cdot \sqrt{P_{n,r}R_{SA}} \ [(\mathrm{A/m})/\sqrt{\mathrm{Hz}}] \quad (9)$$

The measured equivalent magnetic field strength is listed in Table III, comparing the cooled and the room temperature cases. The cooling has changed the property of probe materials slightly. This change is reversible.

The driving power P_d is not the same when the probe is cooled and at room temperature. This is caused by a small frequency dependence of the cables losses, as the resonance frequencies shift slightly. It is also caused by a small variation of the tracking generator's output power at different frequencies. However, the small difference of driving power has no effect on the system probe factor, since the system probe factor is normalized with respect to the driving power, normalizing to 1 volt driving voltage at a 50Ω resistor.

If we take the GPS probe as an example, the received signal increases by 0.8 dB when the probe is cooled. At the same time, the noise power density decreases by 3.89 dB/Hz. The higher sensitivity and the lower noise power density result in an increased sensitivity of 4.69 dB. When this value is converted to the equivalent field strength, the minimal detectable equivalent field strength is 4.8 $(nA/m)/\sqrt{Hz}$ lower when the probe is cooled. Similar improvements are seen for the other probes when cooled.

VI. Conclusion

The change of the system sensitivity by cooling near field probes for the GSM, GPS and WiFi bands using liquid nitrogen has been investigated. We observed increasing Q-factor, higher sensitivity, larger output power, and lower noise power density of the probe system at lowered temperature. The sensitivity of the system, defined as the signal strength at which the SNR is equal to 0 dB improved by 3-6 dB. The cooled probe system is helpful for detecting low electromagnetic fields coupled to RF antennas.

TABLE III
Equivalent Magnetic Field Strength Measured by Probes under Different Temperatures

		T_{room}	T_{LN2}	Difference
GSM Probe	f_c	883.3 MHz	908.6 MHz	25.3 MHz
	P_d	-40.41 dBm	-40.49 dBm	0.08 dB
	P_r	-34.67 dBm	-31.80 dBm	2.87 dB
	$P_{n,r}$	-138.14 dBm/Hz	-141.44 dBm/Hz	3.3 dB/Hz
	SPF	0.3482 (A/m)/V	0.2477 (A/m)/V	0.1005 (A/m)/V
	H_{eq}	9.65 (nA/m)/$\sqrt{Hz}$	4.7 (nA/m)/$\sqrt{Hz}$	6.25 (nA/m)/$\sqrt{Hz}$
GPS Probe	f_c	1562 MHz	1614 MHz	52 MHz
	P_d	-40.78 dBm	-40.90 dBm	0.12 dB
	P_r	-37.38 dBm	-36.58 dBm	0.8 dB
	$P_{n,r}$	-140.03 dBm/Hz	-143.92 dBm/Hz	3.89 dB/Hz
	SPF	0.4404 (A/m)/V	0.3953 (A/m)/V	0.0451 (A/m)/V
	H_{eq}	9.81 (nA/m)/$\sqrt{Hz}$	5.61 (nA/m)/$\sqrt{Hz}$	4.8 (nA/m)/$\sqrt{Hz}$
WiFi Probe	f_c	2470 MHz	2548 MHz	78 MHz
	P_d	-41.2 dBm	-41.19 dBm	0.01 dB
	P_r	-35.32 dBm	34.29 dBm	1.03 dB
	$P_{n,r}$	-139.35 dBm/Hz	-141.46 dBm/Hz	2.09 dB/Hz
	SPF	0.3118 (A/m)/V	0.2753 (A/m)/V	0.0365 (A/m)/V
	H_{eq}	7.51 (nA/m)/$\sqrt{Hz}$	5.20 (nA/m)/$\sqrt{Hz}$	3.19 (nA/m)/$\sqrt{Hz}$

Acknowledgment

This material is based upon work supported by the National Science Foundation under Grant No. 0855878.

References

[1] T. Sudo, H. Sasaki, N. Masuda, and J. L. Drewniak, "Electromagnetic interference (EMI) of system-on-package (SOP)," *IEEE Trans. Adv. Packag.,* vol. 27, no. 2, pp. 304–314, May 2004.

[2] X. Dong, S. Deng, T. Hubing, and D. Beetner, "Analysis of chip-level EMI using near-field magnetic scanning," in *Proc. IEEE Int. Symp. Electromagn. Compat.*, 2004, vol. 1, pp. 174–177.

[3] Y. Gao and I. Wolff, "A new miniature magnetic field probe for measuring 3-dimensional fields in planar high frequency circuits," *IEEE Trans. Microw. Theory Tech.*, vol. 44, no. 6, pp. 911–918, Jun. 1996.

[4] Y. Gao and I. Wolff, "Miniature electric near-field probes for measuring 3-D fields in planar microwave circuits," *IEEE Trans. Microw. Theory Tech.*, vol. 46, no. 7, pp. 907–913, Jul. 1998.

[5] X. Dong, S. Deng, D. Beetner, T. Hubing, and T. P. Van Doren, "Determination of high frequency package currents from near-field scan data," in *Proc. IEEE Int. Symp. Electromagn. Compat.*, 2005, vol. 2, pp. 679-683.

[6] T. Harada, N. Masuda, and M. Yamaguchi, "Near-field magnetic measurement and their application to EMC of Digital equipment," *IEICE Trans. Electron*. vol. E89-C, no. 1, pp. 9-15, Jan. 2006.

[7] S. Lin, S. Yen, W. Chen, and P. Cheng, "Printed magnetic field probe with enhanced performances," in *Proc. IEEE Int. Symp. APMC*, 2009, pp. 649-652.

[8] H. Funato and T. Suga, "Magnetic near-field probe for GHz band spatial resolution improvement technique," in *Proc. IEEE Int. Symp. EMC-Zurich*, 2006, pp. 284-287.

[9] H. Tsutagaya and S. Kazama, "A high sensitive electromagnetic field sensor using resonance," in *Proc. IEEE Int. Symp. EMC*, 2008, pp. 1-6.

[10] H. Chuang, G. Li, E. Song, H. Park, H. Jang, Y. Zhang, D. Pommerenke, and J. Fan, "A magnetic-field resonant probe with enhanced sensitivity for RF interference applications," *IEEE Trans. EMC,* vol. PP, issue: 99, pp. 1-8, Mar. 2013.

[11] D. I. Hoult and R. E. Richards, "The signal-to-noise ratio of the nuclear magnetic resonance experiment," *Journal of Magnetic Resonance*, 24, 71-85, 1976.

[12] P. Styles and N. F. Soffe, "A high-resolution NMR probe in which the coil and preamplifier are cooled with liquid Helium," *Journal of Magnetic Resonance*, 60, 397-404, 1984